38th AIAA/ASME/SAE/ASEE Joint Propulsion Conference & Exhibit
7-10 July 2002, Indianapolis, Indiana

MEASUREMENT OF SOLID PROPELLANT WEB THICKNESS CHANGE DURING COMBUSTION BY X-RAY DIAGNOSTICS

AIAA 2002-3867

Shin-ichiro Tokudome[*], Hiroshi Hasegawa[†],
Masahisa Hanzawa[‡], Masahiro Kohno[§]
[*‡]Institute of Space and Astronautical Science, Sagamihara, JAPAN
[†§]Tokai University, Hiratsuka, JAPAN

ABSTRACT

A new X-ray diagnostic system has been developed for a non-intrusive measurement of the local recession of solid propellant web thickness. The technique utilizes the X-ray absorption characteristics strictly depending on the propellant thickness. A small motor containing two propellant slabs called DSM (Double Slab Motor) is employed, which has a large L/D and designed to have a rectangular port cross-section. X-ray supplied from two sources placed apart from the motor is to be introduced to the motor interior and led to the eight X-ray sensors attached to the motor at its opposite side through the Al windows. Gathered X-ray intensity data are reduced to the local propellant web thickness changes by referring to the *in situ* calibration data obtained otherwise in advance. The resulted local propellant web thickness changes will well contribute to investigate the erosive burning effects in detail.

INTRODUCTION

Erosive burning[1] is a phenomenon that the burning rate of solid propellant can be augmented by the interaction between the reaction fields of the propellant and the gas flows parallel to the propellant burning surfaces. In the case of the solid propellant motors with internal burning grain, erosive burning apparently appears when the mass flux in a grain port is beyond a threshold and the chamber pressure increases. Hence the motor with larger L/D (Length to Diameter Ratio) enhances the chamber pressure rise due to erosive burning early in the firing.

Many theoretical and experimental studies have been conducted on erosive burning so far. Any satisfactory and comprehensive models available for predicting the erosive effect with high accuracy, however, have not been proposed yet since it has been difficult to develop the mathematical model and to justify it quantitatively. For this difficulty there are two major explanations: erosive burning is a complex physicochemical phenomenon induced by the interaction between the combustion fields of solid propellant and the turbulent flow fields in the vicinity of the propellant combustion surfaces; and any techniques has not been accomplished for measuring a local burning rate enhanced under burning condition.

For this reason, the authors have developed a new X-ray diagnostic system[2,3], with the objective of obtaining the better understanding of erosive burning. The system consists of a small solid motor with large L/D and an X-ray diagnostic system to measure the propellant web thickness during combustion. The motor has a peculiar configuration to control the motor combustion pressure and the mass flux in the port. The propellant grain of two propellant slabs that are loaded in parallel face to face and their two parallel combustion surfaces form the port with a rectangular cross section. Varying the nozzle throat diameter and the initial gap between the slabs can control the motor combustion pressure and the mass flux in the port respectively. The non-intrusive X-ray diagnostic system, which was built by utilizing the X-ray absorption characteristics of homogeneous materials, realized continuous measurement of the local propellant thickness under burning conditions.

The experimental results show that the proposed diagnostic system made simultaneous measurement of the chamber pressure and the propellant web thickness possible.

EXPERIMENTAL APPARATUS

Fig. 1 shows a schematic of the experimental setup. A solid motor and two X-ray sources are placed on a test stand in a lead X-ray shield. The authors have developed the small solid motor for studying the erosive burning of composite propellants in detail. Fig. 2 shows a schematic of the motor. It consists of 4 main components made of stainless and soft steels; motor case body with a cylindrical form, forward closure with a residence space of igniter gas, nozzle assembly being one with aft closure, a pair of propellant supports for loading the propellant and fitting the X-ray sensors.

[*] Research Associate, Propulsion Division, Member AIAA.
[†] Researcher, School of Engineering.
[‡] Professor School of Engineering.
[§] Professor, Propulsion Division, Member AIAA Professor.

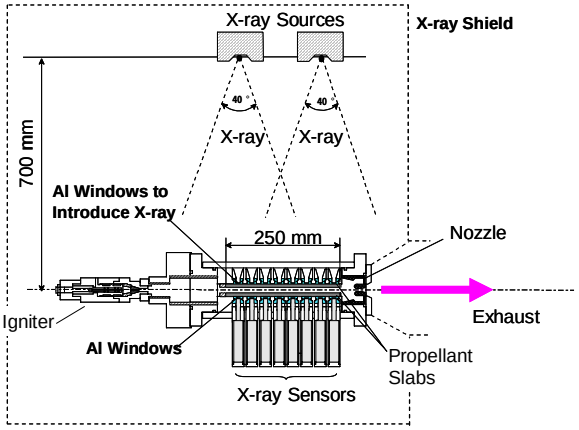

Fig. 1 Schematic of experimental set up

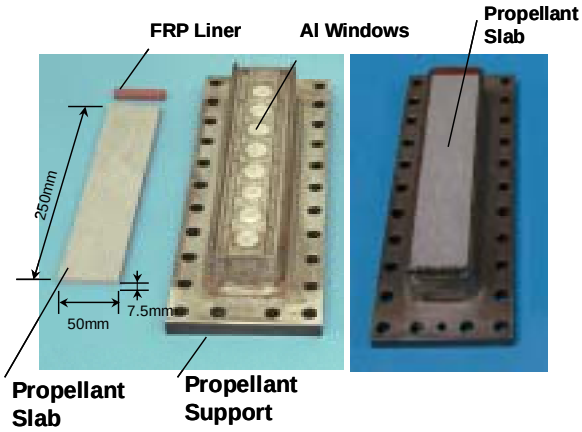

Fig. 3 Propellant supports and propellant slabs

Both of the propellant supports mounted on the top and the bottom of the motor, are removable and each of them houses one of the propellant slabs. Both of the propellant supports have eight Aluminum windows, which have a diameter of 10 mm and a thickness of 3 mm. They are arranged at intervals of 30 mm in the direction of motor axis. The propellant slabs 250 mm long by 50 mm wide by 7.5 mm thick are glued on the propellant supports. The propellant supports and the propellant slabs are shown in Fig. 3. Varying the height of the supports can control the mass flux of in the port. The authors prepared two sets of the propellant supports with different height. They give 5 and 10 mm in the initial gap between the propellant slabs. Because of a peculiar structure like this, we named the motor Double Slab Motor (DSM).

The igniter employed in DSM is a small pyrogen igniter loaded a Polyester/AP composite propellant. Ignition delay characteristics of solid motors using pyrogen igniter can usually express the following empirical correlation:

$$\dot{m}_{ig}{}^{0.8}\tau_{ig}{}^{0.5} = kV_f{}^{2/3} \qquad (2\text{-}1)$$

where $\dot{m}_{ig}$, τ_{ig}, and V_f represent mass flow rate of igniter combustion gas, ignition delay of motor, and motor free volume respectively. As the free volume increases, the ignition delay grows longer. So the ignition can be obtained just on the igniter burnout. This was realized by providing the residence space of igniter gas of 300 cm^3 and optimizing the igniter gas flow rate for each firing condition. By means of this ignition system, erosive burning effect is not affected by an igniter gas flow early in the firing.

A longitudinal section of the nozzle insert is shown in Fig.2. It is submerge shape design to control the combustion product of condensed Al/Al_2O_3 mixture adhering to inner surface of the nozzle throat. Relatively large condensed Al/Al_2O_3 particles not flowing with gas can be trapped in the hollow around the nozzle. In spite of this peculiar

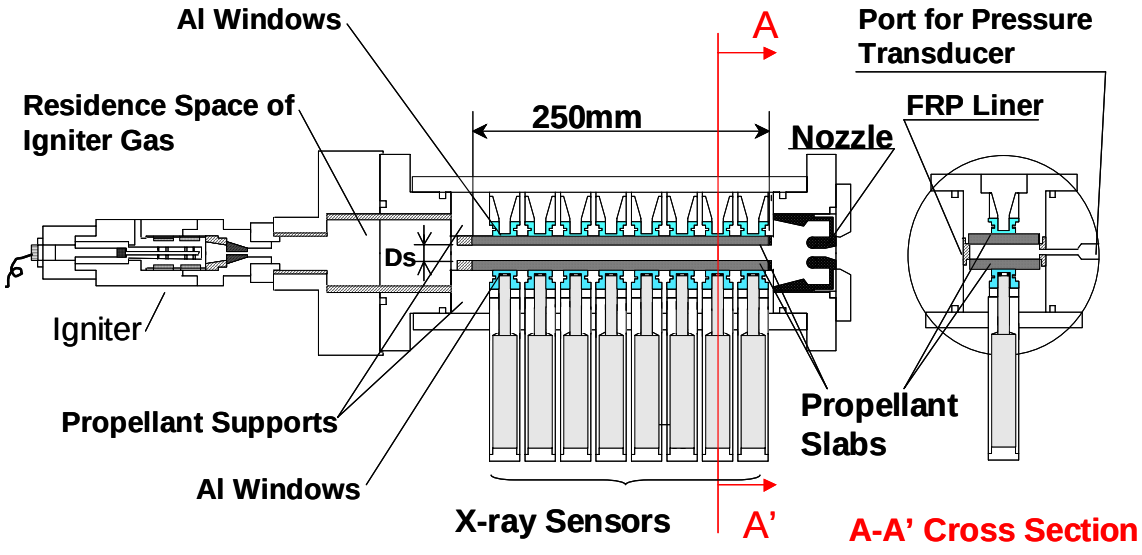

Fig. 2 Double Slab Motor (DSM)

design, nozzle throat area gradually shrinks during the motor operation. In ISAS, this shrinking phenomenon has been known to remarkably occur for a few seconds after ignition in the small size motors for practical use. To avoid systematic error due to this phenomenon, we measured the throat area before and after the firing using an optical profile projector (Nikon V-24B), and also applied a data processing method to estimating a history of nozzle throat area At and a mean characteristic exhaust velocity C* at a time.

Eight scintillation counters (S2226, OHYO KOKEN KOGYO Co., Ltd.) are fitted to the propellant support mounted on the bottom of the motor. The Al windows and ϕ3 perforated Pb disks for controlling the incident X-rays are put between them. They have quick response of the order of 1 microsecond to the incident radiant rays.

Two X-ray apparatus (RXB-100, TORECK Co., Ltd.) are arranged in the direction of the motor axis about 700 mm above DSM that fixed horizontally to a vertical test bench. Their relative position is finely adjusted to be as equal as possible the quantity of the incident X-ray fluxes to the eight X-ray windows. The X-ray is radiated at a divergence cone angle of 40 degree from the each X-ray source. Both of the X-ray apparatus are tuned 100 kV in tube voltage and 2 mA in tube current.

All the experimental apparatus including DSM, two X-ray sources, and eight scintillation counters are set up in a Pb X-ray shield, which is made of a thick steel and thin steel plates mounted Pb plates on to prevent the X-ray from leaking out.

There are three regular measurement items in the firing test. They are eight points of X-ray intensity, static pressures at the forward and aft end in the chamber of DSM, and a chamber pressure of the igniter. The outputs voltages from the sensors are recorded on the Digital Audio Tape (DAT) at the sampling rate of 12 kHz. The digital data are reproduced in a personnel computer at the sampling rate of 1 kHz. Those will be used for the data processing later.

MEASUREMENT OF LOCAL PROPELLANT THICKNESS CHANGE BY X-RAY DIAGNOSIS

The correlation between the X-ray intensity detected and the local propellant thickness is derived from the result of an *in situ* calibration to measure the intensity of the X-ray transmitted for various propellant thicknesses at every measurement position

The *in situ* calibration is conducted in advance of every firing test. We fix a pair of imitative propellant slabs, which made of the same propellant material as we used in the firing tests, in turns. We prepared seven pairs of imitative propellant slabs with various different thicknesses for the calibrations. They are from 2 to 8 mm at intervals of 1 mm in thickness. We measure the thickness of the propellant slab with a micrometer, which has the minimum scale of 10 micron. The scattering of measured values of several measurements with the micrometer is evaluated to be about 30 micron. The X-ray intensity detected at each measurement position is represented by each sensor output voltage Vs, which is amplified with the DC amplifier. The relationship between the X-ray intensity detected and the total thickness of the propellant slabs $(w_1 + w_2)$ obeys the Lambert's Law.

$$V_s = V_{s0} \exp\left[-\mu(w_1 + w_2)\right] \qquad (3\text{-}1)$$

where V_{s0} and μ represents the sensor output voltage proportional to the X-ray intensity and absorption coefficient respectively. μ is not constant for white X-ray and decreases gradually in proportion to the thickness of X-ray transmitted.

A typical result on the *in situ* calibration at the most forward position (Pos. 1) for X-ray measurement is shown in Fig. 4. *w* represents the averaged local propellant thickness defined as the following:

$$w = \frac{1}{2}(w_1 + w_2) \qquad (3\text{-}2)$$

In this figure, the digital data, which were filtered out the oscillation element in high-frequency band over 50 Hz are shown. There are distinct oscillation elements below 50 Hz overlapping with stable mean outputs. The noise reappears well and can be expressed properly by Gaussian distribution function not depending on the position and the slab thickness. A relative error due to the noise was evaluated to be 1 % in three times as standard deviation.

$$\sigma_V = \pm 1\% \qquad (3\text{-}3)$$

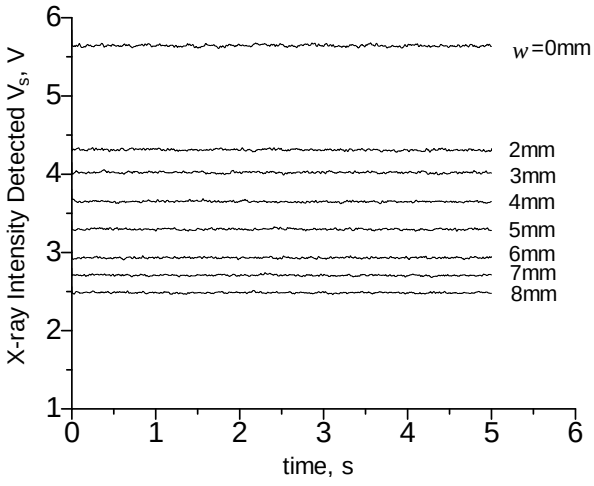

Fig. 4 Typical result of *in situ* calibration

Fig. 5 shows the relationship between *Vs* and 2*w* plotted on semi-logarithmic plane. The absorption coefficient μ is the reciprocal of the slope of the correlation. A Correlation curve, which is obtained by the method of least square with approximately expressing μ as a linear function of the total thickness 2*w*, agrees well with the all calibration data.

$$-\mu = A + B(2w) \qquad (3\text{-}4)$$

We convert the measured value of *Vs* into the instantaneous value of 2*w* in DSM from the calibration curve assumed equation (3-4). In this case, we improved the accuracy and the reliability with correcting the error due to the output drift and the small fluctuation of the amplifier gain by modifying the output to fit it to the calibration curve just before and just after the firing tests.

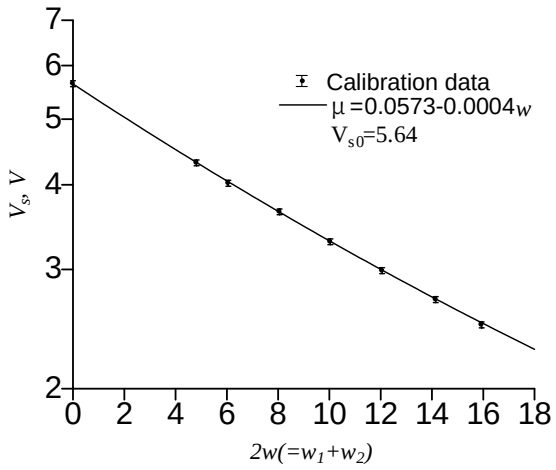

Fig. 5 Relationship between *Vs* and *2w*

Substituting $V_s = \overline{V_s}(1 \pm \sigma_V)$ and Eq. (3-2) into Eq. (3-1), we obtain the following equation:

$$2w = 2\overline{w} \pm \delta(2w) = -\frac{1}{\mu}\ln\frac{\overline{V_s}}{V_{s0}} - \frac{1}{\mu}\ln(1 \pm \sigma_V) \qquad (3\text{-}5)$$

where $2\overline{w}$, $\delta(2w)$ represent a true value and an error of total propellant thickness, and $\overline{V_S}$ represents a true value of sensor output voltage. A measurement error in the propellant slab thickness, therefore, can be expressed as follows:

$$\Delta(2w) = -\frac{1}{\mu}(1 \pm \sigma_V) \approx \pm\frac{\sigma_V}{\mu} \qquad (3\text{-}6)$$

With the assumptions of $\sigma_V = 0.01$ and $\mu = 0.05$, we can evaluate the accuracy of the measurement to be $\Delta(2w) = \pm 0.2$ mm.

Hence, the accuracy of the measurement in averaged propellant slab thickness *w* is ± 0.1mm .

The condition on the path transmitting the X-ray in the firing test is different from that in the *in situ* calibration with two reasons. The one is the presence of combustion product between the slabs the other is that there are thin glue layer between the Al windows and the slabs.

The result of a verification test[4] shows that the change in the X-ray intensity due to presence of the combustion product of condensed phase was negligible. We can also neglect the influence of the glue layer because it is less than 0.2 mm in thickness and less than half of the propellant in density.

Since the bulk modulus of the propellant can be considered to be almost infinity as good as the rubber materials for general use, the change in the propellant density due to the chamber pressure is negligible.

EXPERIMENTAL RESULTS

The test condition is listed in Table 1. Table 2 shows the composition and the combustion properties of the propellant.

Table 1 Test conditions

Nozzle throat Diameter D_t, mm	9.1
Chamber Pressure P_c [1)], MPa	5
Initial Propellant Gap D_s, mm	5
Maximum Mass Flux G_{max} [1)],kg/m^{2}s	800

1) No Erosive Burning

Table 2 Propellant properties

Propellant	**BP-206J**
Composition, % by mass	
Oxidizer(NH_4ClO_4)	**69**
Binder(HTPB)	**17**
Metal Fuel(Al)	**14**
Density ρ_p, g/cm^3	**1.7**
Linear Burning Rate r_b [1)], mm/s	**4.7**
Pressure Exponent n	**0.378**
Adiabatic Flame Temp. T_f [2)] ,K	**3031**
Mean Molecular Wt. W_m [2)] ,g/mol	**25.4**
Specific Heat Ratio γ [2)]	**1.194**

1)@5MPa, 20deg 2)frozen equilibrium calculation @5MPa

Fig. 6 shows typical chamber pressure histories under the condition of a 5 mm in the initial gap Ds between the propellant slabs. Fig. 7 shows typical results of the measurement of the averaged local propellant web thickness at 27mm downstream (Pos.1) and 237mm downstream (Pos.8). The pressure histories in Fig. 6 show that the ignition system operated properly and favorable ignition was made. We can also describe measured combustion surface distributions in longitudinal direction as a parameter of the time in Fig. 8.

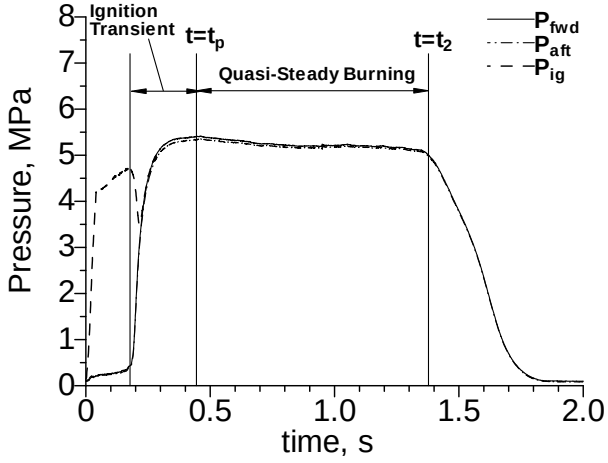

Fig. 6 Chamber pressure histories

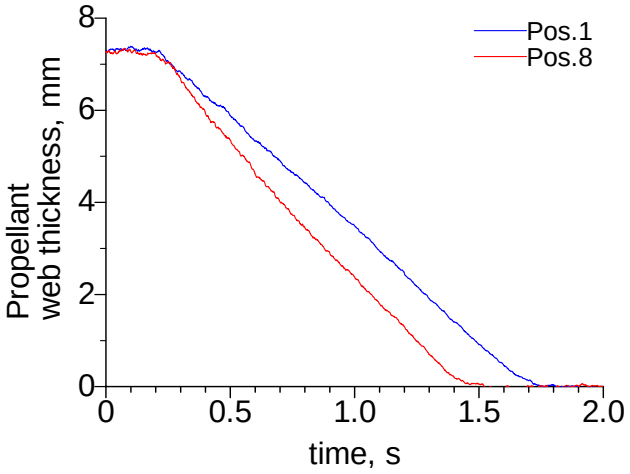

Fig. 7 Propellant web thickness change at Pos.1 and Pos.8

Erosive burning effect is usually distinguished early in the firing with smaller port area, so that a chamber pressure peak appears in a transition from the ignition transient to the steady burning. When the pressure peak appears at the time t_p after motor ignition, the regression of combustion surfaces averages 1.3 mm from the initial surface and the propellant is consumed 18 % of the total loading mass. In the quasi-steady burning period just after the t_p, the combustion surface is inclined in the longitudinal direction because a burning rate of the propellant becomes higher toward the aft end of the grain. This indicates the erosive burning effects.

The authors also conducted a combustion-interrupted test to verify the accuracy of the X-ray diagnostic system. A burning interruption was accomplished by means of the extinction induced by rapid depressurization, which was performed by separating a nozzle assembly fixed to DSM with two pyrotechnic bolts in a moment. Injecting the gas nitrogen (GN_2) into the chamber just after operating the two pyrotechnic bolts

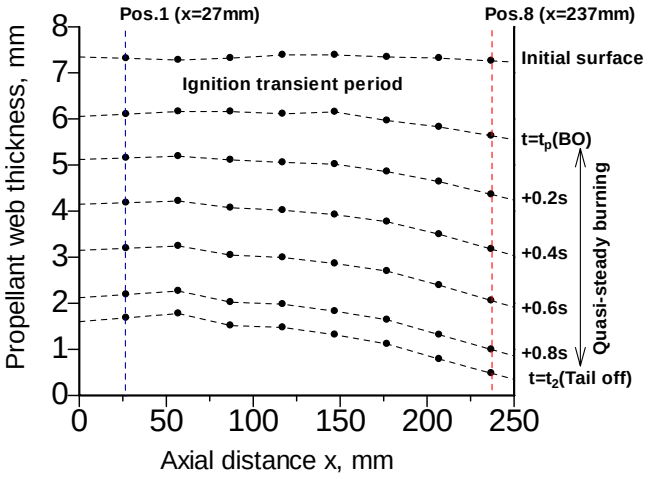

Fig. 8 Combustion surface distributions in the direction of motor axis

controlled a reignition. Propellant thicknesses before and after the combustion tests were directly measured with micrometer with an accuracy of 0.01 mm.

The results for measured chamber pressure and local propellant thickness by X-ray diagnostics are shown in Fig. 9. Fig. 10 shows axial distributions of the burnt propellant thickness averaged in the lateral direction measured with direct measurement and with X-ray diagnostic system. The measured values by two different methods almost agree.

The thicknesses of remained propellant slabs were directly measured at a total of 90 points, at 18 points in the longitudinal direction and at 5 points in the lateral direction respectively. Results for the measured propellant thickness showed that the propellant thickness distributions in the lateral direction were almost uniform, so that the scatterings were within 0.2 mm. Differences between the two slabs in the thickness along the motor central axis were less than 0.1 mm from their own averaged values. This indicates the propriety of the method of estimating the propellant slab thickness at the average value of the two slabs.

The larger errors at the 3rd and 4th positions are due to weak X-ray in these measuring positions because the relative positions of the X-ray sources had not been optimized yet. After that, the positions were optimized and the measuring accuracy at all the positions were improved higher level mentioned above.

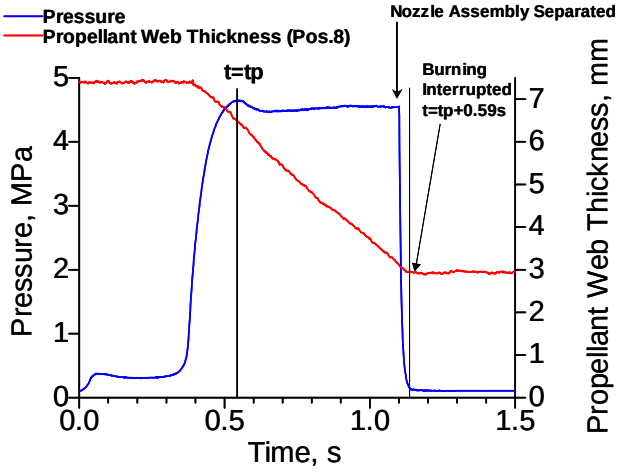

Fig. 9 Measured chamber pressure and propellant web thickness in combustion interrupted test

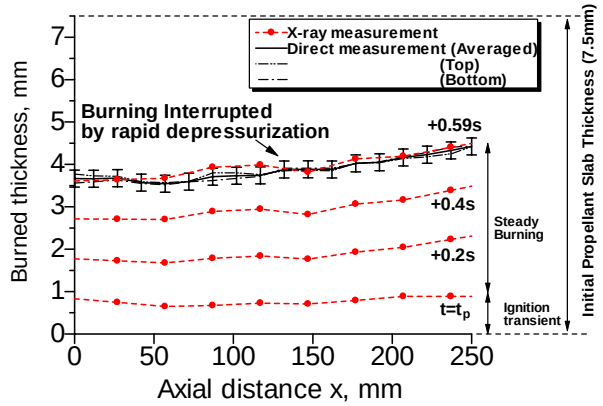

Fig. 10 Comparison of measured propellant web thickness distribution

CONCLUSIONS

Usefulness of the X-ray diagnostics was demonstrated to measure the propellant local recession behavior during the DSM firing. The data gathered here will well contribute to the further progress in the study of the erosive burning..

The accomplished X-ray diagnostics has also been successfully applied to the investigation of the PDL (Pressure Deflagration Limit) of composite propellants and their linear burning rate characteristics at lower pressure near Pdl.

ACKNOWLEDGEMENTS

The authors would like to thank all the people who participated in the design and development of the experimental apparatus for their help.

The authors were assisted in conducting experiments by Mr. Akihide Kitasaka in Tokai Giken Co.,LTD, Mr. Kazumi Murata in TORECK Co.,LTD, Mr. Yoshio Seike in NOF Co., and Mr. Kiyokazu Kobayashi. The authors would like to express their special thanks to them.

The authors also would like to express their thanks to Dr. Angelo Volpi in TEMPE-CNR for his useful suggestions in developing the X-ray diagnostic system.

REFERENCES

[1] Green, L. Jr., “Erosive Burning of Some Composite Solid Propellants,” Jet Propulsion, Vol. 24, 1954, pp. 9-15.

[2] Kohno, M., Volpi, A., Tokudome, S., Nagata, H. and Kimura, M., “Experimental Study on Erosive Burning in a Slab Motor by X-Ray Diagnostics,” 20th ISTS, 1996, Vol.1, pp.13-18.

[3] Kohno, M., Volpi, A., Tokudome, S., ”X-Ray Diagnostics for Local Burning Rate Measurement of Solid Propellant,” 4th Inter. Symp. on Special Topics in Chemical Propulsion, Stockholm, 1996.

[4] Kohno, M., Tokudome, S., Kobayashi, K., Hasegawa, H. and Nojiri, T., “Solid Propellant Burning Rate Measurement by use of X-ray Absorption Characteristics (in Japanese),” Symp. on Space Transportation , ISAS, 1999.